

# PIXE and pXRF Comparison Analysis of a Mockup Canvas Painting

## Análise Comparativa de PIXE e pXRF de um Simulado de Pintura em Tela

Carlos Roberto Appoloni<sup>1</sup>; Fabio Lopes<sup>2</sup>; Marcia de Almeida Rizzuto<sup>3</sup>; Augusto Camara Neiva<sup>4</sup>; Renato Akio Ikeoka<sup>5</sup>; Marcia Rizzo<sup>6</sup>

### ABSTRACT

For the purposes of comparison among different equipments and laboratories involved in atomic-nuclear methodologies applied in arts and archaeometry, a special mockup canvas painting was made with dozens of pigments of different colors and varnishes of different types and manufacturers. This study evaluate two different XRF equipment and PIXE methods as complementary tools to examine canvas paintings. Twenty-four inorganic substances of this mockup canvas were measured in three different laboratories, LEC, LFNA, and LAMFI for the identification of the key elements. In this paper, net count ratios and standard percentage deviations between lines are shown, as well as examples of sensibility to low-content elements that can be used for distinguishing pigments, and a comparison of the penetration of these techniques. The results show the differences between the pXRF and PIXE methodologies and between the two pXRF geometry/equipments employed.

**keywords** pXRF, PIXE, canvas, painting, pigments

### RESUMO

Para fins de comparação entre diferentes equipamentos e laboratórios envolvidos em metodologias atômico-nucleares aplicadas em artes e arqueometria, foi confeccionado um mimético em tela com dezenas de pigmentos de cores diferentes e vernizes de diferentes tipos e fabricantes, com o objetivo de avaliar dois diferentes equipamentos de XRF e a metodologia PIXE como ferramentas complementares para examinar pinturas em tela. Vinte e quatro substâncias inorgânicas deste mimético foram medidas em três laboratórios diferentes, LEC, LFNA e LAMFI para a identificação dos elementos-chave. No presente artigo, são mostradas razões de contagem líquida e desvios percentuais padrão entre linhas, bem como exemplos de sensibilidade para elementos de baixo teor que podem ser usados para distinguir pigmentos, e também uma comparação da penetração dessas técnicas. Os resultados mostram as diferenças entre as metodologias pXRF e PIXE e também entre as duas geometrias/equipamentos pXRF empregados.

**palavras-chave** pXRF, PIXE, tela, pintura, pigmentos

Received: February 28, 2023

Accepted: October 04, 2023

Published: November 27, 2023

<sup>1</sup>Prof. Dr., Dept. Physics, UEL, Londrina, PR, Brazil. E-mail: appoloni@uel.br

<sup>2</sup>Dr., Dept. Physics, UEL, Londrina, PR, Brazil. E-mail: fabiolopes@uel.br

<sup>3</sup>Prof. Dr., Dept. Physics, USP, São Paulo, SP, Brazil. E-mail: rizzuto@usp.br

<sup>4</sup>Prof. Dr., Dept. Physics, USP, São Paulo, SP, Brazil. E-mail: acneiva@usp.br

<sup>5</sup>Prof. Dr., Dept. Physics, UEL, Londrina, PR, Brazil. E-mail: ikeoka@uel.br

<sup>6</sup>Dr. EBA, UFRJ, Rio de Janeiro, RJ, Brazil. E-mail: mrizzo@eba.ufrj.br

## Introduction

The use of non-destructive elemental spectroscopic methods such as X-ray fluorescence spectroscopy and Particle-Induced X-ray Emission (PIXE) is becoming common in the area of art and cultural heritage objects, helping the characterization of the constituents of the artwork as well as the identification of the deterioration processes, in order to choose the better method to conserve them. These techniques are very powerful and important in material characterization, especially for pigments identification (Calligaro et al., 2015; Caridi et al., 2022; de Viguierie et al., 2010; Hunt & Speakman, 2015; Molari & Appoloni, 2023; Rizzuto et al., 2014; Shaaban et al., 2009) and for the determination of layers composition and thickness (Neelmeijer et al., 2000).

Strengths of pXRF are the possibility of *in situ* and non-invasive fast measurements, whereas PIXE requires a much more expensive accelerator facility for laboratory measurements and EDS requires sample removal and preparation, and an expensive equipment compared with pXRF (Calligaro et al., 2015; Rizzuto et al., 2014).

However, as XRF and PIXE techniques are not usually able to identify elements with atomic numbers below 13, pigments are usually not identified by their complete composition, but rather by some key elements. The main purpose of the present study is to verify the sensibility of two Portable X Ray Fluorescence spectroscopy (PXRF) equipment and one PIXE equipment for the identification of the key elements of some important artistic pigments when applied to a typical canvas painting. For this, a mimetic of a canvas painting was constructed trying to cover as much as possible the materials used by painters in antiquity. This paper presents the results of the analysis of twenty-four pigments in this canvas painting, measured in three different laboratories in Brazil: Laboratório de Eletroquímica e Corrosão (LEC), Laboratório de Física Nuclear Aplicada (LFNA) and Laboratório de Análise de Materiais por Feixes Iônicos (LAMFI).

## Materials and methods

### Mockup canvas preparation

The mockup painting, Figure 1, a complex creation specially prepared for this type of work, was made by Márcia Rizzo on a lined canvas stretched over a stretcher wood. With the exception of three strips on the sides of the canvas, its entire surface received a priming layer with a mixture of animal glue and calcium carbonate ( $\text{CaCO}_3$ ), as those used by old artists. Over this preparation layer, a standard paint was made using different types of pure pigments,

mixed of pigments, inclusions of metals (Ag and Au foils and pieces of metal), alternate layers of pigments and foils, and different kinds of varnishes, totaling six layers of materials. Paraloid B72 dissolved in Xylene was used as a binder. The proportion of Paraloid was approximately 30% in Xylene. The pigments were mixed with this solution to form a dispersion (paint). The solution and pigment(s) were mixed in a proportion of 50%. The strips in the left and upper sides, without any preparation underlayer, were divided into approximately 40 rectangles, which were covered with different kinds of organic materials and metal foils used by the artists. The bottom side strip was painted with different antique and modern paints and pigments. The mockup was not subject to any type of aging or treatment, and the paints were analyzed after the mockup was completely dry. The twenty-four inorganic pigments presented in this paper belong to the bottom strip or to the central area of the mockup.

**Figure 1** - Mockup canvas painting (34×42 cm).



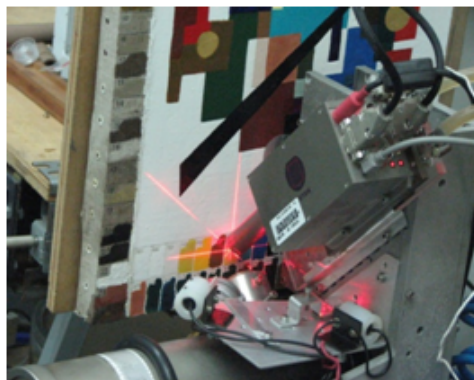
### Particle induced X-ray emission - PIXE

PIXE measurements were performed at the Laboratory of Analysis of Materials with Ion Beams (LAMFI-USP). It was used a Van de Graaff accelerator at the Institute of Physics of the University of São Paulo. In this setup, a 6- $\mu\text{m}$  aluminum foil is used as a vacuum window. The painting was placed 6 mm from the vacuum window, and the beam energy at the sample surface was 2.37 MeV (2.6 MeV internal beam energy) with a resolution of 14 keV. The X-ray detector was placed 55 mm from the sample, and the solid angle was geometrically calculated to 2 msr (a collimator was used to restrict the solid angle to avoid the Ar signal from the air). The X-ray detector resolution is 160 eV (FWHM@MnK $\alpha$ ). The system was set to measure each spectrum over 600 seconds (Rizzuto et al., 2005). Experimental set up is shown at Figure 2.

**Figure 2** - PIXE experimental set up at LAMFI. The number of some different colors areas are visible.



**Figure 4** - pXRF experimental set up at LEC.



### Portable X-ray fluorescence - pXRF at LFNA

The setup of pXRF equipment installed at the Applied Nuclear Physics Laboratory (Appoloni et al., 2007; Parreira et al., 2019), located at the State University of Londrina in southern Brazil (<http://www.uel.br/grupos/gfna>), consists of a mini X-ray tube (Moxtek, Inc., 4 W, Ag target) and a Si-drift detector model X123 (Amptek, Inc.) with resolution of 185 eV.

A special Ag filter with a  $100\mu\text{m}$  thickness was used to absorb low energy radiation and an Ag collimator with a 3 mm diameter aperture was applied to diminish the incident radiation that comes from the canvas (Figure 3).

The tube was operated using a 35kV and  $5\mu\text{A}$ , with 300s of excitation-detection time, and geometry was set at  $45^\circ/45^\circ$ , Figure 3.

**Figure 3** - pXRF experimental set up at LFNA.



### Portable X-ray fluorescence - pXRF at LEC

A semi-portable EDXRF (transportable) spectrometer (Neiva et al., 2006) installed at Laboratório de Eletroquímica e Corrosão (LEC) in the Escola Politécnica da Universidade de São Paulo, composed by an X-ray tube with W anode and a Si-drift Ketek X-ray detector was applied, Figure 4.

Both incident and detection angles to the painting surface were  $45^\circ$ , as can be seen in Figure 4. Given this constraint, the geometry was planned so that the air gap between the painting and the detector was as small as possible to minimize absorption by the atmosphere. The incident X-ray beam was collimated to a diameter of 1.5 mm. The X-ray tube was operated at 55 kV, 1.0 mA with a 1.5mm collimator. Each spectrum was taken for 500s.

## Results

Table 1 shows the list of the measured pigments. Table 2 presents the count ratios between two key elements for each pigment and employed laboratory/technique, where is possible to see the large sensibility differences for the various elements among the employed techniques and equipments, considering also the different composition of the pigments.

One observes that the ratios are quite different for PIXE and pXRF. Ti-K/Ca-K ratio for pigment 45, for instance, is around 40-100 times larger for PIXE than for XRF. This is due to the larger PIXE sensibility at low energies, when compared to pXRF, which makes PIXE more efficient for light elements than pXRF.

On the other hand, pXRF is more efficient for medium and heavy elements than PIXE. This explains the differences between the two methods in ratios observed for the key elements of the pigments.

There is also a small difference of ratios between the two pXRF results. It should be attributed to the different excitation sources (W-tube and Ag-tube, respectively), to the different use of filters (no filter and Ag-filter, respectively), to different detector efficiency curves, and so on.

One should comment that, when operated at high enough maximum energies, PXRF allows a good detection of K-peaks of elements like Sn, Sb, and Cd, which are present in several pigments.

**Table 1** - Measured pigment regions and their number in the painting, grouped by color.

Paint number area at the mockup	Pigment commercial name	Molecular formula
45	Titanium White	TiO <sub>2</sub>
48	Zinc Yellow	CrO <sub>4</sub> Zn
49	Cadmium Yellow medium	CdS
50	Indian Yellow	C <sub>19</sub> H <sub>18</sub> O <sub>11</sub> Mg. 5H <sub>2</sub> O
51	Naples Yellow light	Pb <sub>3</sub> (SbO <sub>4</sub> ) <sub>2</sub>
52	Cobalt-Turquoise Blue	CoO.Al <sub>2</sub> O <sub>3</sub>
53	Cerulean Blue	CoO.nSnO <sub>2</sub>
54	Phthalocyanin Greenish Blue	Cu(C <sub>32</sub> H <sub>16</sub> N <sub>8</sub> )
55	Artificial Ultramarine Blue	Na <sub>8-10</sub> .Al <sub>6</sub> Si <sub>6</sub> O <sub>24</sub> S <sub>2-4</sub>
56	Ultramarine Violet	Al <sub>6</sub> Na <sub>6</sub> O <sub>24</sub> S <sub>8</sub> Si <sub>6</sub>
57	Violet Lac	CH <sub>2</sub> OCOCH <sub>3</sub>
58	Magenta Lac	C <sub>2</sub> OH <sub>12</sub> N <sub>2</sub> O <sub>2</sub>
59	Manganese Violet	(NH <sub>4</sub> ) <sub>2</sub> Mn <sub>2</sub> (P <sub>2</sub> O <sub>7</sub> ) <sub>2</sub>
60	Cadmium Red medium	CdHgS <sub>2</sub>
61	English Red	Fe <sub>2</sub> O <sub>3</sub> +CaCO <sub>3</sub>
62	Iron Red	Fe <sub>2</sub> O <sub>3</sub>
63	Vermilion	HgS
64	Red Cinabrian	HgS
65	Cinabrese	clays + Fe <sub>2</sub> O <sub>3</sub>
68	Ultramarine Green	2NaAlSiO <sub>4</sub> Na <sub>2</sub> S
74	Raw Umber	Fe <sub>2</sub> O <sub>3</sub> +MnO <sub>2</sub> +H <sub>2</sub> O
76	Cassel Earth	FeO-OH+MnO <sub>2</sub>
77	Black Roman Earth	Fe <sub>2</sub> O <sub>3</sub> +SiO <sub>2</sub> +Al <sub>2</sub> O <sub>3</sub> + CaO + MgO
78	Ivory Black	Ca <sub>3</sub> (PO <sub>4</sub> ) <sub>2</sub> + C + MgSO <sub>4</sub>

The areas of these K-peaks were not presented in Table 2 (L-peaks were shown instead) because they were not recorded in the PIXE measurements. Another important difference between PIXE and XRF is the penetration depth. As the PIXE analysis-thickness is much smaller than that of PXRF, its results are less affected by underlayers. This effect was clearly observed in the spectra of pigment layers painted over the Bone Glue / Calcium Carbonate layer. These underlayers contained high Ca, Sr, and Zn contents. All the pigment spectra obtained with pXRF presented peaks of these elements, see Figure 5.

PIXE spectra, on the opposite, did not present them. However, the PIXE spectrum for pigment 48 presents a

very clear Sr peak. As the other underlayer peaks, Ca and Zn, are not present, one should conclude that in this case, the Sr is present in the pigment layer.

It is important to mention that, although pigments are usually identified by their main elements, sometimes a low-content element can be important for this objective. For instance, the spectra of ultramarine blue (pigment 55, Figures 6 and 7) and ultramarine violet (pigment 56, Figures 8, 9 and 10) are almost similar. However, a small Rb K-peak can be observed only in ultramarine violet, by PXRF (Figures 8 and 9). On the other hand, PIXE allowed the observation of a small K-peak of Cr in ultramarine blue (Figure 7), but not in ultramarine violet (Figure 10).

**Table 2** - Elements count ratios for each pigment and employed laboratory/ technique and respective propagated deviations.

Pigment	Peaks	LEC - pXRF		LFNA - pXRF		LAMFI - PIXE	
		Ratio	Deviation	Ratio	Deviation	Ratio	Deviation
45	Ti-K / Ca-K	3.61	0.38%	9.28	0.83%	398.6	5.9%
48	Zn-K / Cr-K	4.19	0.14%	4.38	0.25%	0.31	0.34%
49	Cd-L / Zn-K	7.39	0.87%	0.87	1.80%	224.2	4.7%
50	Ni-K / Ca-K	6.32	0.38%	8.80	0.20%	4.54	1.7%
51	Pb-L / Sb-L	84.04	0.65%	253.1	1.9%	0.58	0.44%
	Pb-L / Ti-K	58.82	0.57%	21.33	0.60%	0.13	0.36%
52	Zn-K / Co-K	2.16	0.29%	1.96	0.47%	0.52	1.1%
	Zn-K / Ti-K	1.29	0.27%	1.37	0.41%	0.04	0.93%
53	Sn-K / Co-K	0.81	0.40%	0.10	0.98%	4.40	0.45%
54	Cu-K / Ca-K	0.79	0.52%	1.10	0.78%	0.07	1.3%
	Cu-K / Cl-K	4.68	0.87%	7.09	1.6%	0.03	1.3%
55	Fe-K / Ca-K	0.24	1.1%	0.19	1.8%	0.15	2.2%
	Fe-K / K-K	13.44	8.2%	8.55	10.0%	0.46	2.7%
56	Fe-K / Ca-K	1.19	1.7%	0.29	2.2%	0.29	3.2%
	Fe-K / K-K	6.23	4.9%	4.76	7.4%	0.17	3.0%
57	Ca-K / Fe-K	107.6	2.7%	56.65	4.7%	866.4	8.2%
	Fe-K / Cl-K	0.21	3.02%	0.44	4.72%	0.00	8.18%
58	Cu-K / Ni-K	84.21	2.2%	84.54	4.7%	55.05	7.9%
	Cu-K / Fe-K	5.53	0.50%	5.47	0.77%	1.52	1.2%
	Cu-K / Ca-K	1.90	0.35%	2.00	0.50%	0.13	0.78%
59	Mn-K / Ca-K	5.91	0.42%	4.86	0.64%	15.02	1.1%
	Mn-K / P-K	104.53	2.3%	267.59	6.8%	5.55	0.61%
60	Cd-L / Se-K	0.12	0.42%	0.02	1.2%	17.51	1.2%
	Cd-L / S-K	69.28	8.9%	14.14	12.9%	5.85	0.87%
61	Fe-K / Ca-K	3.19	0.33%	5.16	0.47%	0.57	0.36%
62	Fe-K / Ca-K	23.50	0.42%	19.12	0.58%	5.28	0.43%
63	Hg-L / S-K	71.16	0.78%	746.19	5.0%	1.05	1.9%
64	Cd-L / Hg-L	0.02	0.36%	0.02	6.4%	7.55	1.3%
	Cd-L / Ba-L	0.31	0.44%	0.26	6.4%	0.79	0.86%
	Cd-L / S-K	1.18	1.6%	1.07	7.4%	1.29	1.2%
65	Zn-K / Fe-K	13.03	0.36%	14.09	0.58%	0.44	0.67%
68	Ni-K / Co-K	2.61	0.55%	2.34	0.95%	1.47	1.9%
	Ni-K / Cr-K	0.36	0.38%	0.34	0.57%	0.06	1.2%
74	Fe-K / Mn-K	7.07	0.30%	7.22	0.50%	4.41	0.44%
76	Fe-K / Ca-K	0.53	0.41%	0.92	0.50%	0.09	0.38%
77	Fe-K / Ca-K	1.96	0.38%	2.16	0.52%	0.26	0.56%
78	Ca-K / Fe-K	31.66	1.3%	26.52	2.1%	294.89	2.4%

Figure 5 - Effect of underlying layers.

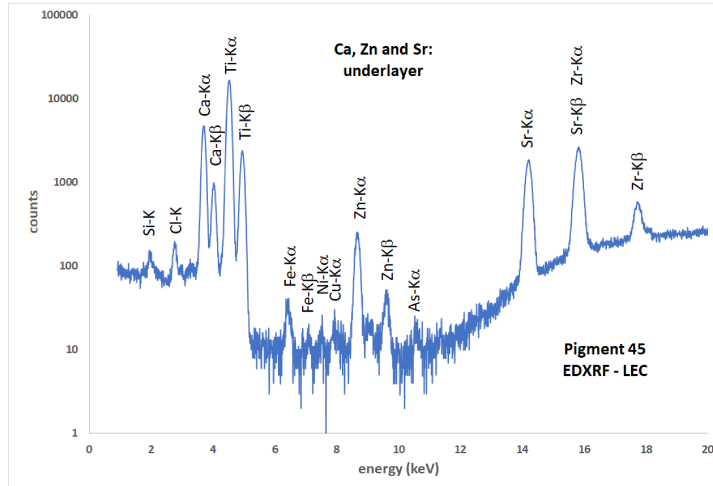


Figure 6 - Ultramarine Blue, LEC / pXRF spectrum.

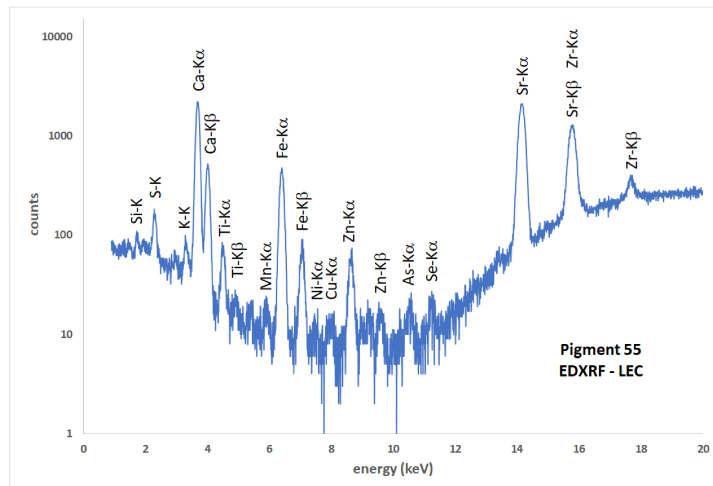


Figure 7 - Ultramarine Blue, LAMFI / PIXE spectrum.

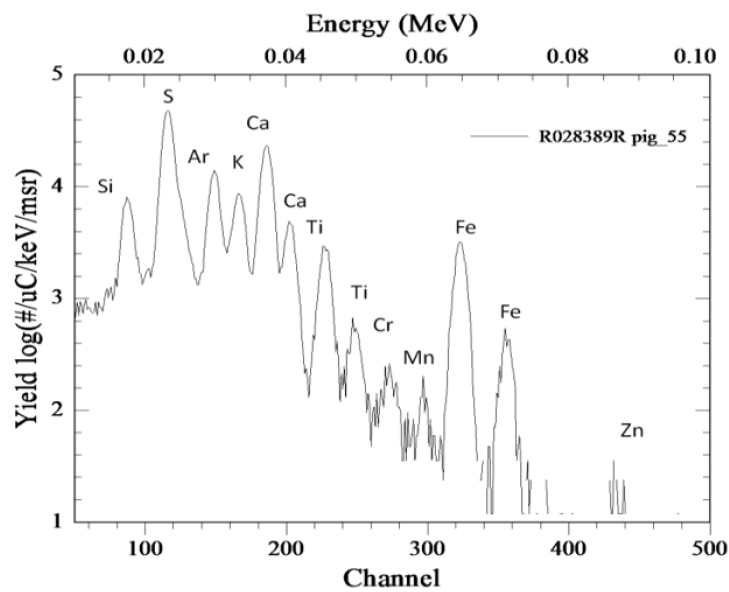


Figure 8 - Ultramarine Violet, LEC / pXRF spectrum.

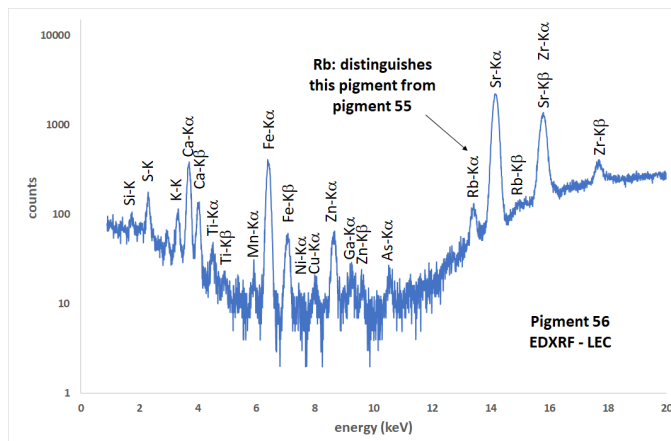


Figure 9 - Ultramarine violet, LFNA / pXRF spectrum.

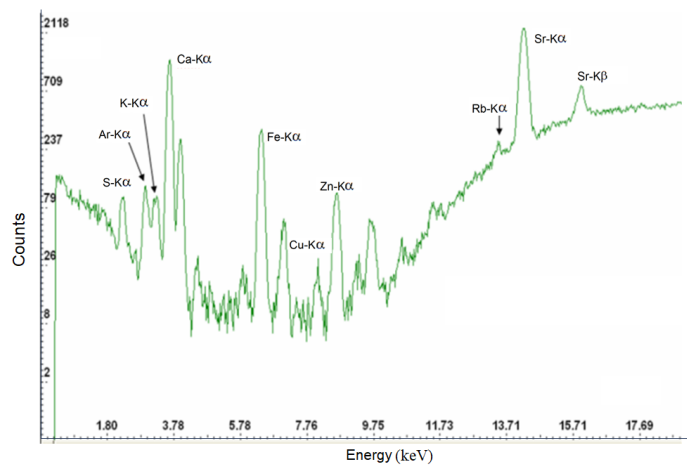
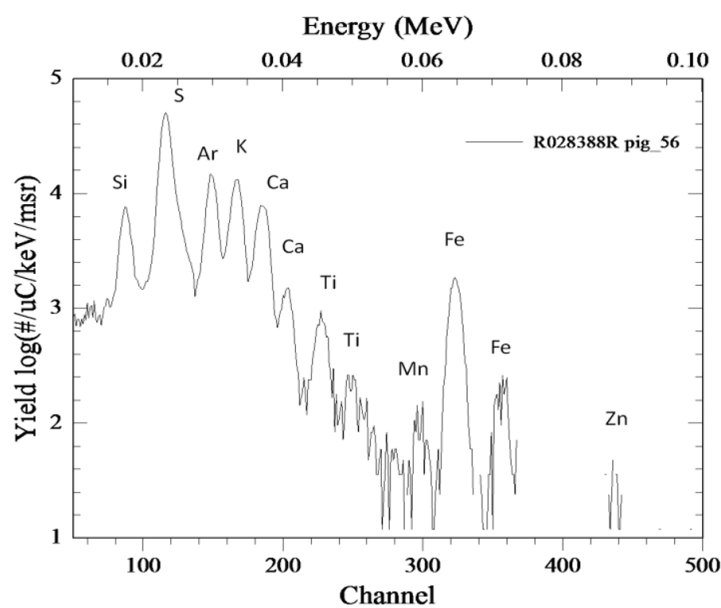


Figure 10 - Ultramarine Violet, LAMFI / PIXE spectrum.



## Conclusions

The constructed mockup of a canvas painting is a very good object for testing different methodologies of painting characterization. The pXRF's and PIXE measurement presented a good complementary analysis of the pigments. The two employed pXRF equipments allowed an interesting comparison between a low-power one, at LFNA, with 175mW, and the LEC system, with 55W. PIXE and XRF are complementary in specific cases. For example, if we need both low-energy lines and high-energy lines from the same element, or from different elements. In the case of the two pXRF, it is possible to avoid misleading escape peaks (e.g., from Fe in samples where it is wanted to measure V or Ti) by changing the excitation voltage or also enhancing some element's relative excitation by changing the X-ray tube anode from Ag to W or vice-versa.

## Author contributions

C.R. Appoloni participated in: supervision, conceptualization, methodology, data curation, analysis, investigation, original draft preparation, writing, review and editing. F. Lopes participated in: data curation, analysis, investigation. M.A. Rizzuto participated in: conceptualization, methodology, data curation, analysis, investigation, writing. A.C. Neiva participated in: conceptualization, methodology, data curation, analysis, investigation, writing. R.A. Ikeoka participated in: data curation, analysis. M. Rizzo participated in: methodology, writing.

## Conflicts of interest

The authors declare no conflict of interest.

## Acknowledgments

Authors acknowledge CAPES, FAPESP and CNPq.

## References

- Appoloni, C. R., Blonski, M. S., Parreira, P. S., & Souza, L. A. C. (2007). Study of the pigments elementary chemical composition of a painting in process of attribution to Gainsborough employing a portable X-rays fluorescence system. *Nuclear Instruments & Methods in Physics Research*, 580(1), 710–713. <https://doi.org/10.1016/j.nima.2007.05.141>
- Calligaro, T., Gonzalez, V., & Pichon, L. (2015). PIXE analysis of historical paintings: Is the gain worth the risk? *Nuclear Instruments and Methods in Physics Research Section B: Beam Interactions With Materials and Atoms*, 363, 135–143. <https://doi.org/10.1016/j.nimb.2015.08.072>
- Caridi, F., Ricca, M., Paladini, G., Crupi, V., Majolino, D., Donato, A., Guido, G., Mantella, G., Randazzo, L., La Russa, M. F., & Venuti, V. (2022). Multi-Technique Diagnostic Investigation in View of the Restoration of “The Glory of St. Barbara” Painting by Mattia Preti. *Applied Sciences*, 12(3), 1385. <https://doi.org/10.3390/app12031385>
- de Viguerie, L., Walter, P., Laval, E., Mottin, B., & Armando Solé, V. (2010). Revealing the sfumato Technique of Leonardo da Vinci by X-Ray Fluorescence Spectroscopy. *Angewandte Chemie*, 49(35), 1–5. <https://doi.org/10.1002/anie.201001116>
- Hunt, A. M. W., & Speakman, R. J. (2015). Portable XRF analysis of archaeological sediments and ceramics. *Journal of Archaeological Science*, 53, 626–638. <https://doi.org/10.1016/j.jas.2014.11.031>
- Molari, R., & Appoloni, C. R. (2023). A study by portable X-ray fluorescence (pXRF) of the painting “Still Life with Vase, Plate and Flowers” (1886–1888). *Applied Radiation and Isotopes*, 196, 110779. <https://doi.org/10.1016/j.apradiso.2023.110779>
- Neelmeijer, C., Brissaud, I., Calligaro, T., Demortier, G., Hautajarvi, A., Mader, M., Martinot, L., Schreiner, M., Tuurnala, T., & Weber, G. (2000). Paintings—a challenge for XRF and PIXE analysis. *X-Ray Spectrometry*, 29(1), 101–110. [https://doi.org/10.1002/\(SICI\)1097-4539\(200001/02\)29:1<101::AID-XRS413>3.0.CO;2-A](https://doi.org/10.1002/(SICI)1097-4539(200001/02)29:1<101::AID-XRS413>3.0.CO;2-A)
- Neiva, A. C., Dron, J. N., & Lima, S. C. (2006). Considering spurious peaks in the EDXRF analysis of metallic pre-Columbian pieces of the Museum of Ethnology and Archaeology of the University of Sao Paulo. In A. Ruiz-Conde, M. Arjonilla-Álvarez, P. J. Sánchez Soto, G. Durán Domínguez, & J. C. R. Cabello (Coords), *Heritage, Weathering & Conservation: Proceedings of the International Conference on Heritage, Weathering and Conservation* (pp. 605–611). Taylor & Francis.
- Parreira, P. S., Melquiades, F. M., Lopes, F. L., Oliveira, V. F., & Appoloni, C. R. (2019). *Sistema portátil de Fluorescência de Raios X* (BR Patent 0801331-4).

- Rizzutto, M. A., Tabacniks, M. H., Added, N., Barbosa, M. D. L., Curado, J. F., Santos, J., W. A., Lima, S. C., Melo, H. G., & Neiva, A. C. (2005). The external beam facility used to characterize corrosion products in metallic statuettes. *Nuclear Instruments & Methods in Physics Research Section B: Beam Interactions with Materials and Atoms*, 240(1), 549–553. <https://doi.org/10.1016/j.nimb.2005.06.153>
- Rizzutto, M., Moro, M., Silva, T., Trindade, G., Added, N., Tabacniks, M., Kajiya, E., Campos, P., Magalhães, A., & Barbosa, M. (2014). External-PIXE Analysis for the Study of Pigments from a Painting from the Museum of Contemporary Art. *Nuclear Instruments and Methods in Physics Research Section B: Beam Interactions with Materials and Atoms*, 332, 411–414. <https://doi.org/10.1016/j.nimb.2014.02.108>
- Shaaban, A., Ali, M., Turos, A., Korman, A., & Stonert, A. (2009). PIXE Analysis of Ancient Egyptian Pigments (Case Study). *Journal of Nano Research*, 8, 71–77. <https://doi.org/10.4028/www.scientific.net/JNanoR.8.71>